
Figures and figure supplements

A role for descending auditory cortical projections in songbird vocal learning

Yael Mandelblat-Cerf, et al.

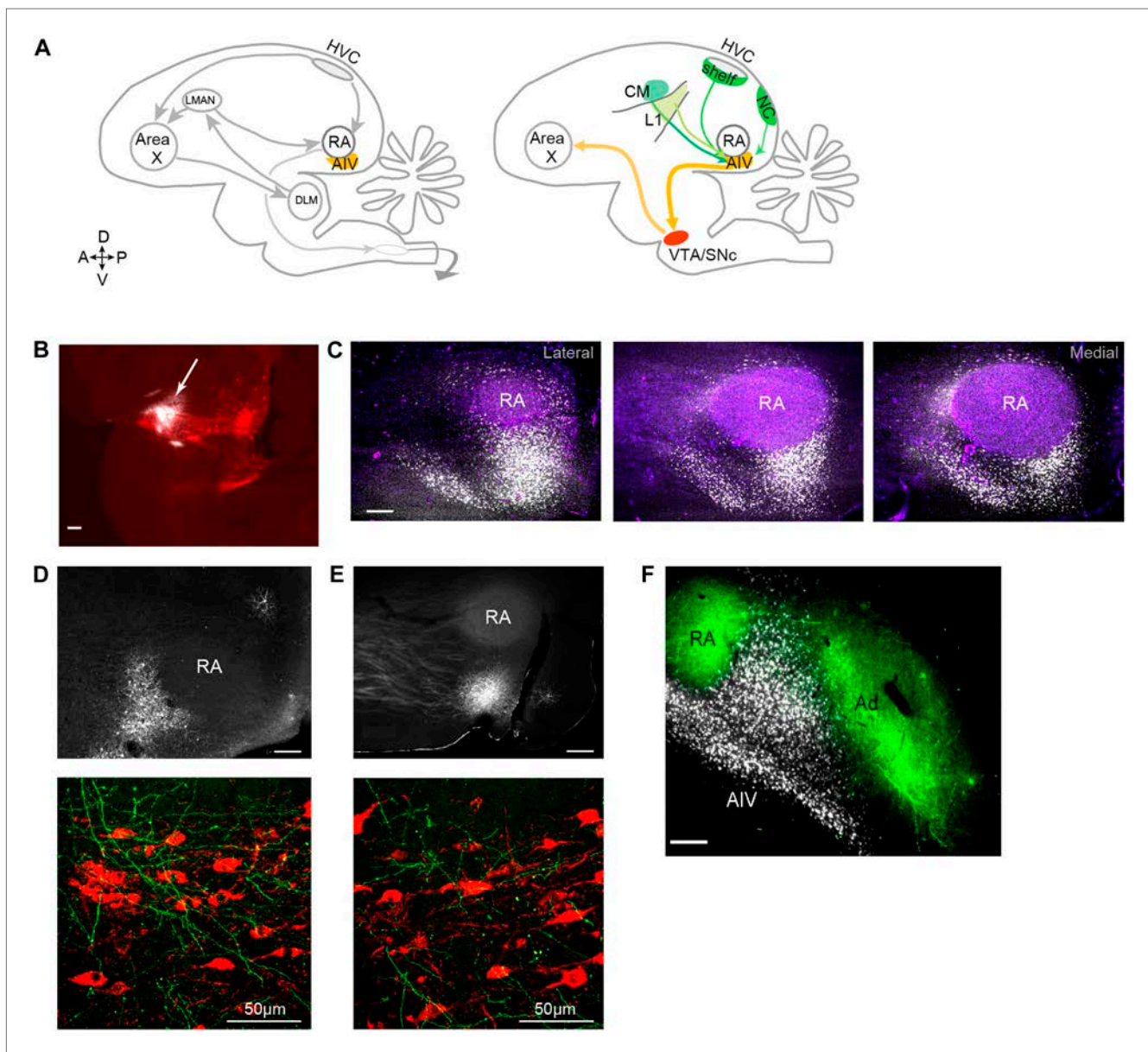


Figure 1. Characterization of avian ‘cortical’ areas projecting to the dopaminergic midbrain. **(A)** Left panel: schematic of the songbird brain (in sagittal view) showing classical song control brain areas. Nuclei HVC and RA form the descending song motor pathway, necessary for song production. Nucleus RA is in the arcopallium, a cortical-like region homologous to layer-5 neurons of the mammalian cortex. Also shown is the anterior forebrain pathway (AFP), a circuit necessary for vocal learning but not vocal production. The AFP consists of a basal ganglia homologue Area X, thalamic nucleus DLM, and cortical-like nucleus LMAN, which projects to RA. Right panel: schematic showing a set of pathways that are the focus of this paper, including a previously described projection to Area X from neurons in the dopaminergic midbrain nuclei VTA and SNc (Gale et al., 2008). Also shown is AIV, a part of the intermediate arcopallium found to project to VTA and SNc. Projections to AIV from auditory cortical areas L1, CM, and HVC-shelf are elucidated here. **(B)** Sagittal section showing the injection site of a retrograde tracer (CTB, white color, arrow) within VTA/SNc (TH-stained neurons, red). **(C)** Three sagittal sections through the arcopallium showing retrogradely labeled neurons in AIV (fluorescence, white) and relation to RA (dark field image, purple). Panel at left is most lateral; sections 200 μ m apart. **(D)** Upper panel: image of injection site of a GFP-expressing virus (HSV, fluorescence white) in the anterior part of AIV, showing relation to RA (dark field image). Bottom panel: sagittal section of VTA/SNc showing anterogradely labeled fibers from AIV (green) and TH-stained neurons (red). **(E)** Same as **D**, with an injection site in AIV ventral to RA. All scale bars 200 μ m unless indicated otherwise. In panels **A–E**, anterior is left; dorsal is up. **(F)** Coronal section showing axons in RA and Ad (green), anterogradely labeled from LMAN and LMAN-shell, respectively (Dextran 10 MW Alexa 488). AIV neurons (white) labeled by injection of a retrograde tracer (CTB) in VTA and SNc (medial, left; dorsal, up).

DOI: 10.7554/eLife.02152.003

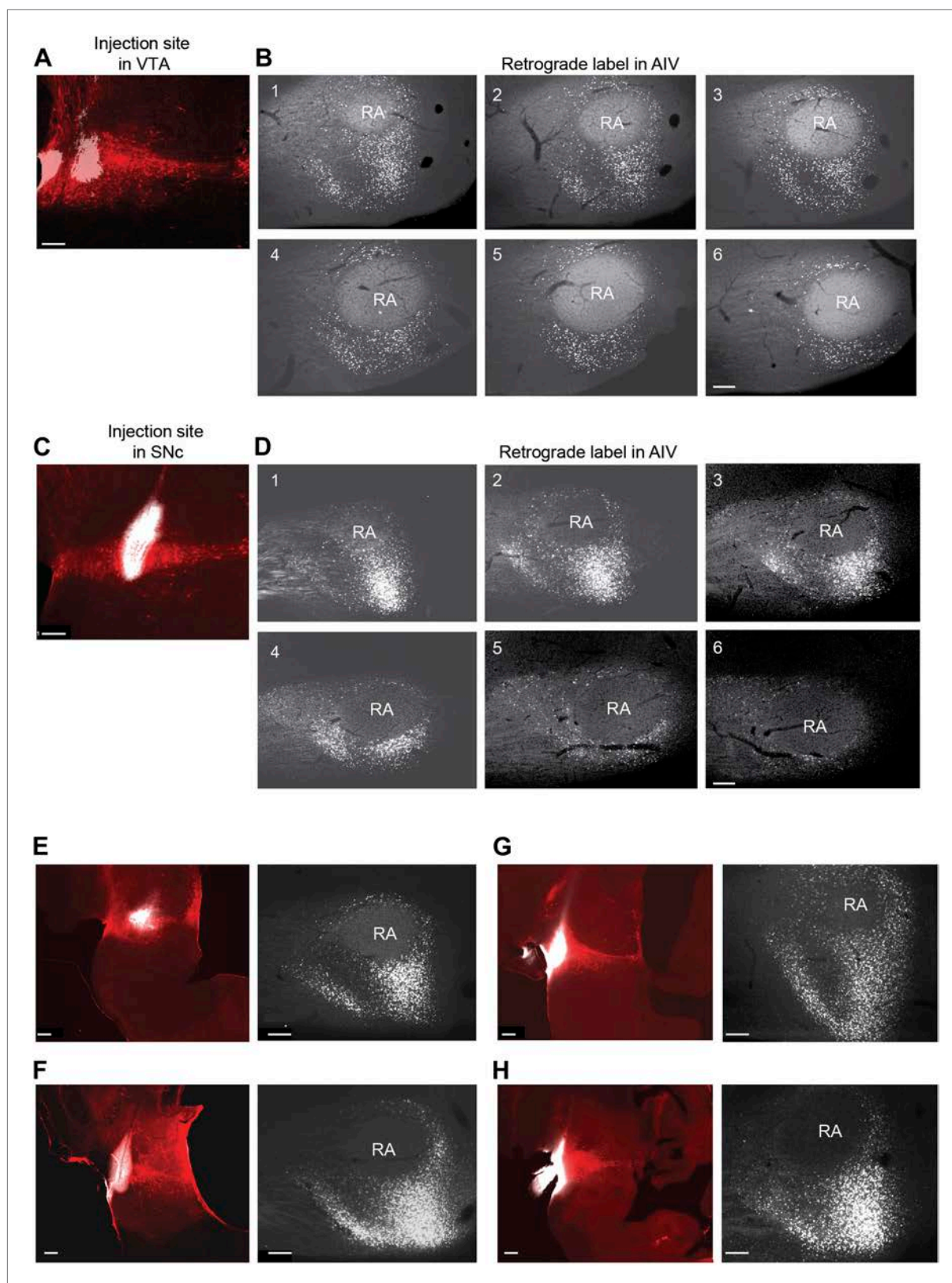


Figure 1—figure supplement 1. Retrograde labeling of AIV neurons from VTA and SNc.

DOI: [10.7554/eLife.02152.004](https://doi.org/10.7554/eLife.02152.004)

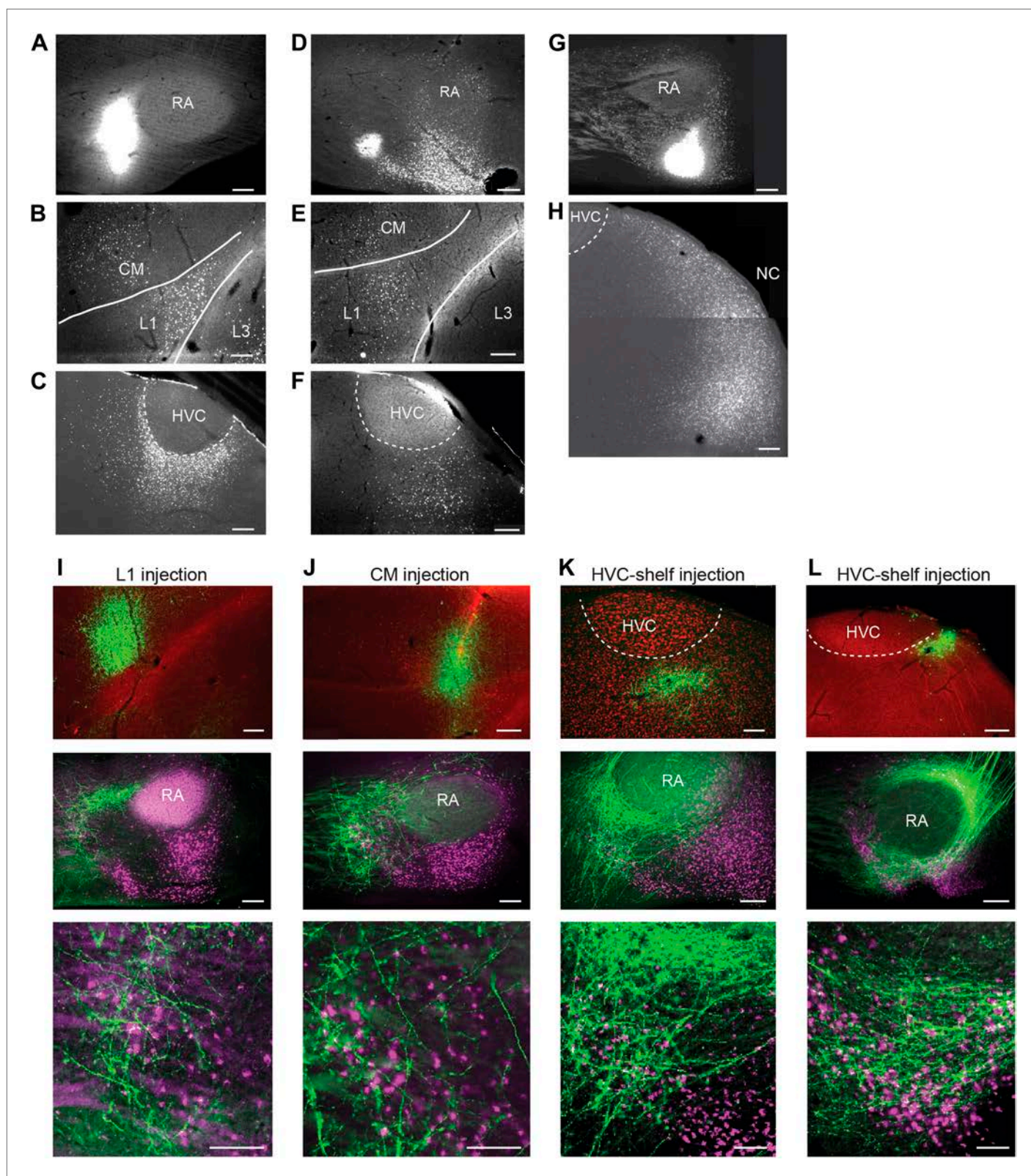


Figure 2. Cortical inputs to ventral intermediate arcopallium (AIV): retrograde and anterograde tracing. **(A)** Injection of a retrograde tracer (CTB) anterior to RA in the vicinity of AIV. **(B)** Retrograde label in cortical auditory areas L1 and CM resulting from the injection shown above. **(C)** Labeled neurons in HVC-shelf of the same bird. **(D–F)** Same as panels A–C. Injection of CTB was targeted to the anterior 'stripe' part of AIV. **(G)** Injection of CTB into the HVC-shelf. **(H)** Retrograde label in cortical auditory areas L1 and CM resulting from the injection shown above. **(I)** Labeled neurons in HVC-shelf of the same bird. **(J)** Same as panels A–C. Injection of CTB was targeted to the anterior 'stripe' part of AIV. **(K)** Injection of CTB into the HVC-shelf. **(L)** Retrograde label in cortical auditory areas L1 and CM resulting from the injection shown above. *Figure 2. Continued on next page*

Figure 2. Continued

posterior part of AIV, directly ventral to RA. **(H)** Retrogradely labeled neurons in caudal nidopallium (NC) resulting from the injection shown above. **(I–L)** Anterograde tracing from auditory cortical areas L1, CM, and HVC-shelf. **(I)** Upper panel— injection of a GFP-expressing virus (HSV, green) into auditory field L1. Middle panel shows labeled axons in the vicinity of AIV neurons retrogradely labeled (purple) from VTA/SNc. Color in RA is due to auto fluorescence, not label. Bottom panel shows higher magnification view from image above. **(J)** Same as **(I)**, but the injection of HSV-GFP was made into the auditory caudal mesopallium (CM). **(K)** Same as **(I)**, but the injection of HSV-GFP was made into HVC-shelf. Scale bars: 100 μm for lower panels of **I–L**; 200 μm for all other panels.

DOI: [10.7554/eLife.02152.005](https://doi.org/10.7554/eLife.02152.005)

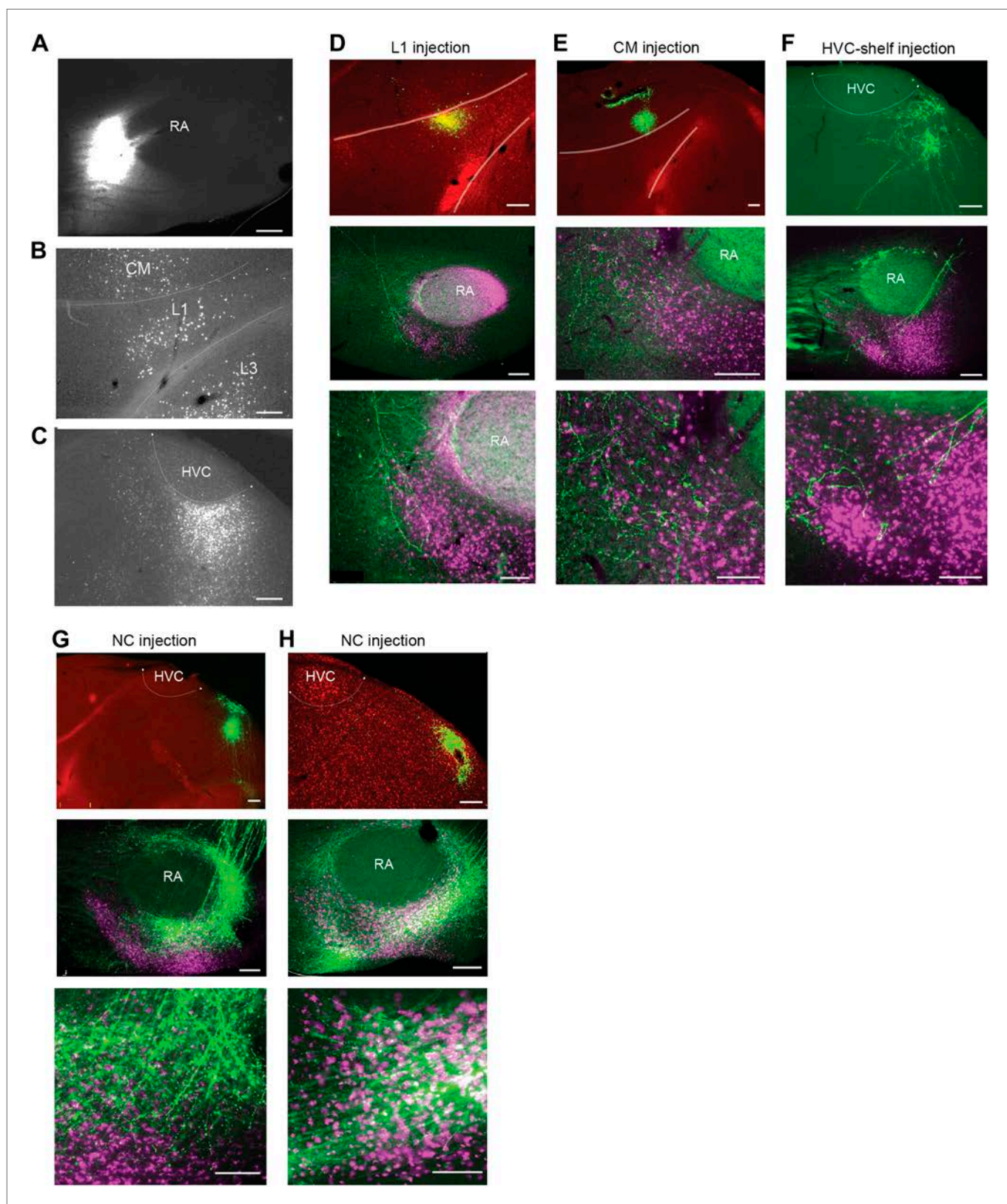


Figure 2—figure supplement 1. Cortical inputs to ventral intermediate arcopallium (AIV).

DOI: [10.7554/eLife.02152.006](https://doi.org/10.7554/eLife.02152.006)

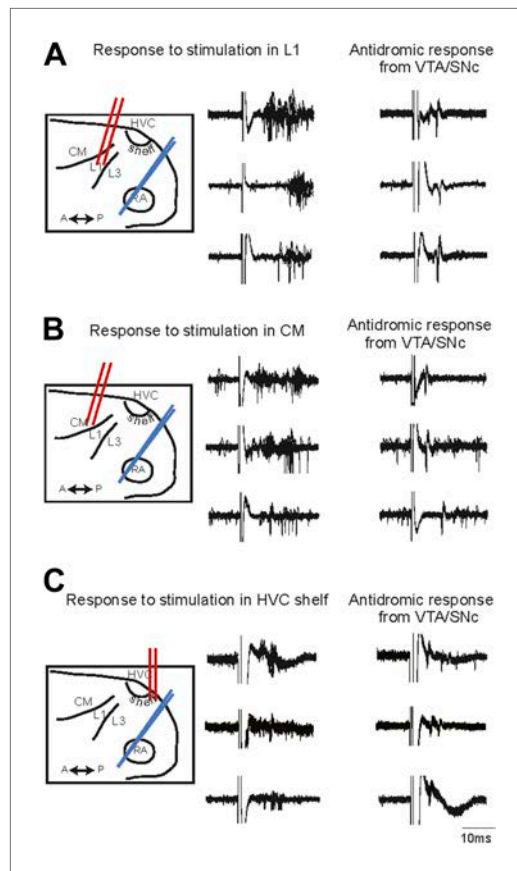


Figure 3. Electrophysiological verification of functional connectivity. Electrical stimulation in auditory cortical areas L1, CM, and HVC-shelf drives spiking in VTA/SNC-projecting neurons in AIV. **(A)** Schematic at left illustrates the location of the stimulating electrodes (red) in L1 and the location of the recording electrode (blue) in AIV. Middle traces: responses of 3 antidromically identified AIV neurons to L1 stimulation (overlaid responses from ten trials). Right traces: antidromic response of the same neurons to electrical stimulation in VTA/SNc. **(B and C)** The panels are analogous to those shown in **(A)**, except the stimulation electrode is placed in caudal mesopallium (CM) or in the posterior part of HVC-shelf.

DOI: [10.7554/eLife.02152.007](https://doi.org/10.7554/eLife.02152.007)

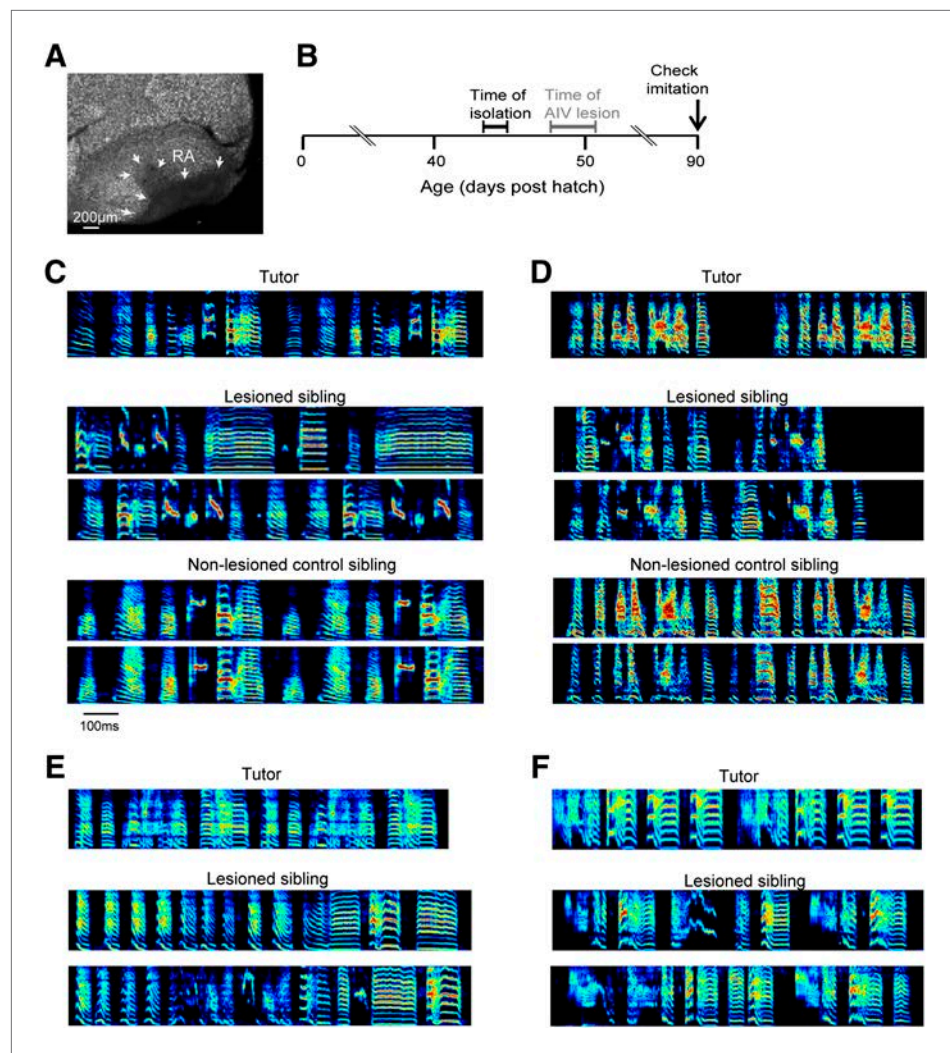


Figure 4. Bilateral lesions of AIV impair tutor imitation. (A) Excitotoxic lesion targeted to AIV by injection of NMA. Lesion borders indicated by arrowheads (sagittal section; anterior left, dorsal up). (B) Schematic timeline of experimental protocol. (C) Song spectrograms of an adult bird (90 dph) that underwent bilateral lesion of AIV as a juvenile, compared to an unlesioned control sibling. Top: spectrogram of tutor song. Middle: two example song spectrograms of the lesioned bird (45% lesion, 0.205 imitation score). Bottom: two example song spectrograms of the control sibling (0.235 imitation score). (D) Same as panel C, but for a different pair of birds (lesioned bird, 66% lesion, 0.1566 imitation score; control sibling, 0.27 imitation score). (E and F) Song spectrograms of two additional adult birds that underwent lesions of AIV as juveniles. These birds did not have control siblings. (Bird in panel E, 61% lesion, 0.097 imitation score; bird in panel F, 77% lesion, 0.114 imitation score.)

DOI: [10.7554/eLife.02152.008](https://doi.org/10.7554/eLife.02152.008)

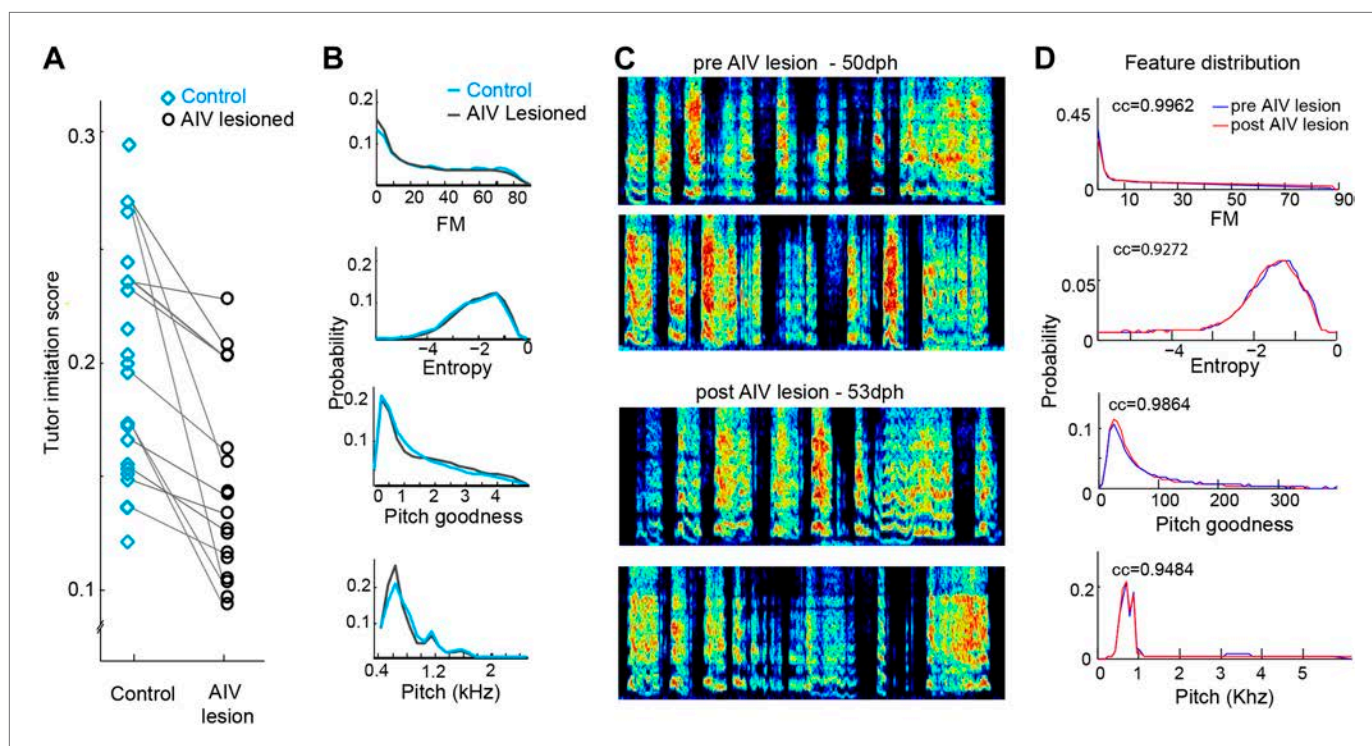


Figure 4—figure supplement 1. Effect of AIV lesions on song motor production and imitation.

DOI: [10.7554/eLife.02152.009](https://doi.org/10.7554/eLife.02152.009)

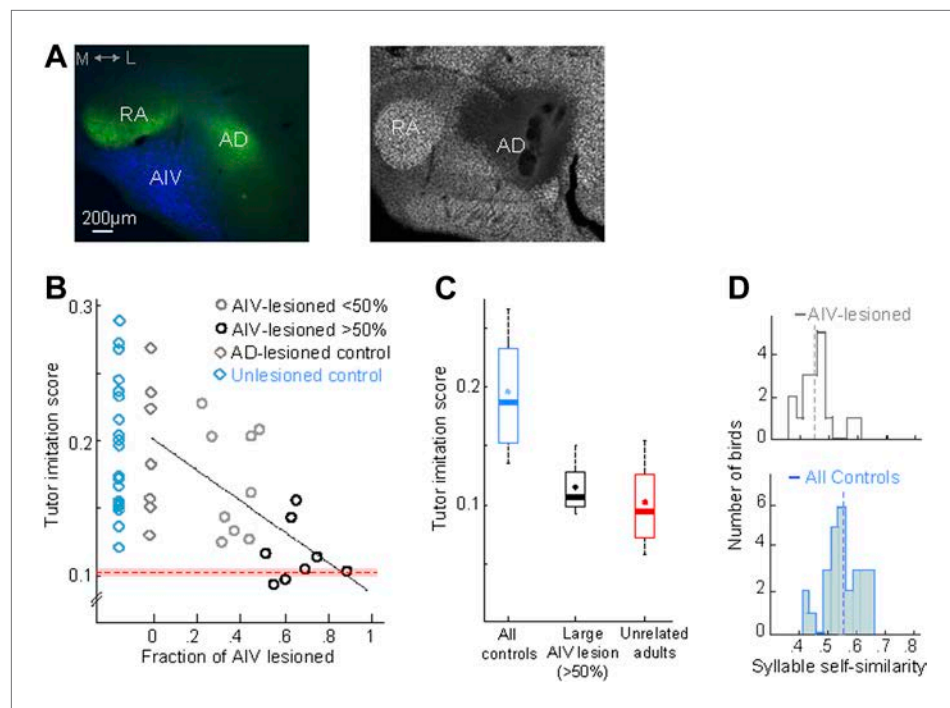


Figure 5. AIV lesions, but not Ad lesions, impair tutor imitation. **(A)** Left: coronal section showing the relation between AIV neurons (retrogradely labeled from VTA/SNc, blue) and nucleus Ad (anterograde labeling from LMAN-shell, green; medial, left; dorsal, up) Right: coronal section showing excitotoxic lesion of Ad, revealed by loss of NeuN staining (white, note that the lesion affected some of the overlying nidopallium). **(B)** Tutor imitation score plotted as a function of the extent of AIV lesion for each bird (hollow circles, $n = 17$ AIV-lesioned birds). Ad-lesioned birds ($n = 7$) are shown as 0% lesion (hollow gray diamonds) since Ad lesions had minimal impact on AIV. No significant impairment of song-imitation was observed in Ad-lesioned birds as compared to unlesioned controls (blue diamonds, $n = 19$ birds). Solid line denotes least square fit to Ad-lesioned and AIV lesioned data points. Red dashed horizontal line indicates mean of all similarity comparisons between 20 unrelated adult birds (red shaded area indicates SEM) **(C)** Boxplot of the distribution of imitation scores of all control birds (cyan, unlesioned, and Ad-lesioned controls) and birds with large AIV-lesions (black, >50% lesion). Also shown is a boxplot of the distribution of similarity scores of all pairwise comparisons between 20 unrelated adult birds (red). Whiskers denote 10–90 percentile. Asterisk in each boxplot denotes the mean, heavy line denotes median. **(D)** Distribution of syllable self-similarity in AIV-lesioned birds (top) and in control birds (bottom, unlesioned, and Ad-lesioned controls combined). Dashed lines denote mean of distributions.

DOI: [10.7554/eLife.02152.010](https://doi.org/10.7554/eLife.02152.010)

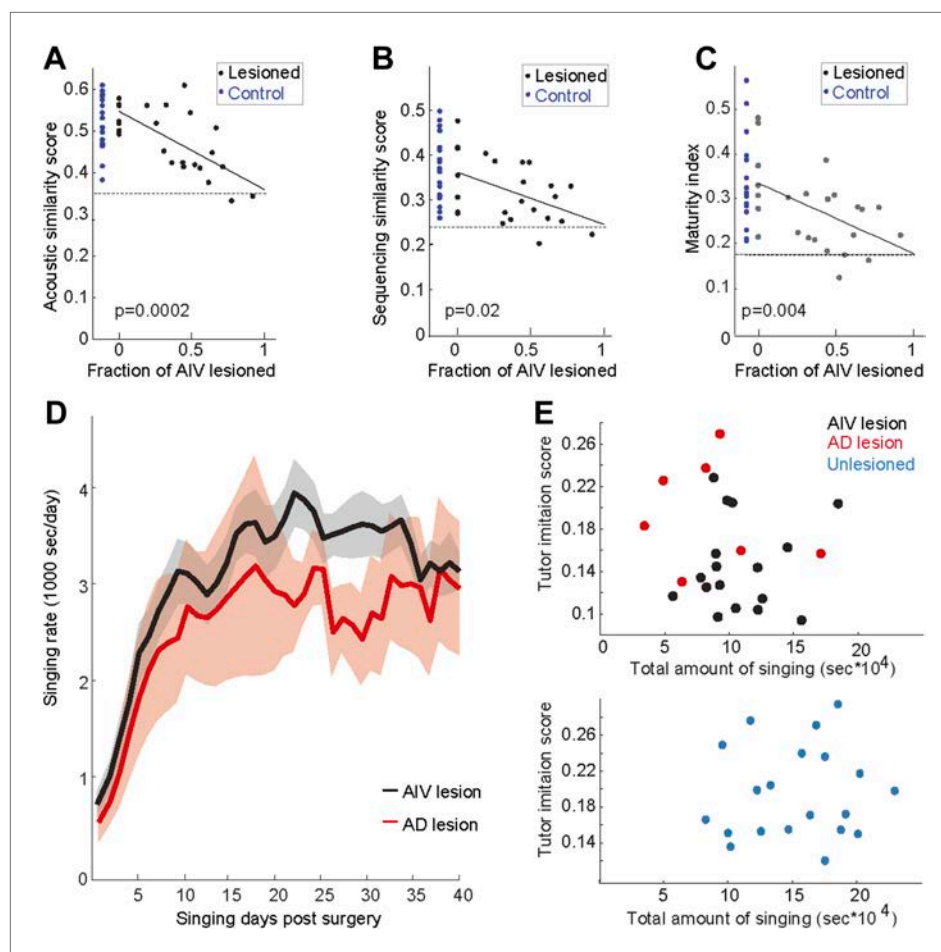


Figure 5—figure supplement 1. Effect of AIV lesions on song imitation, development of song stereotypy, and rate of singing.

DOI: [10.7554/eLife.02152.011](https://doi.org/10.7554/eLife.02152.011)

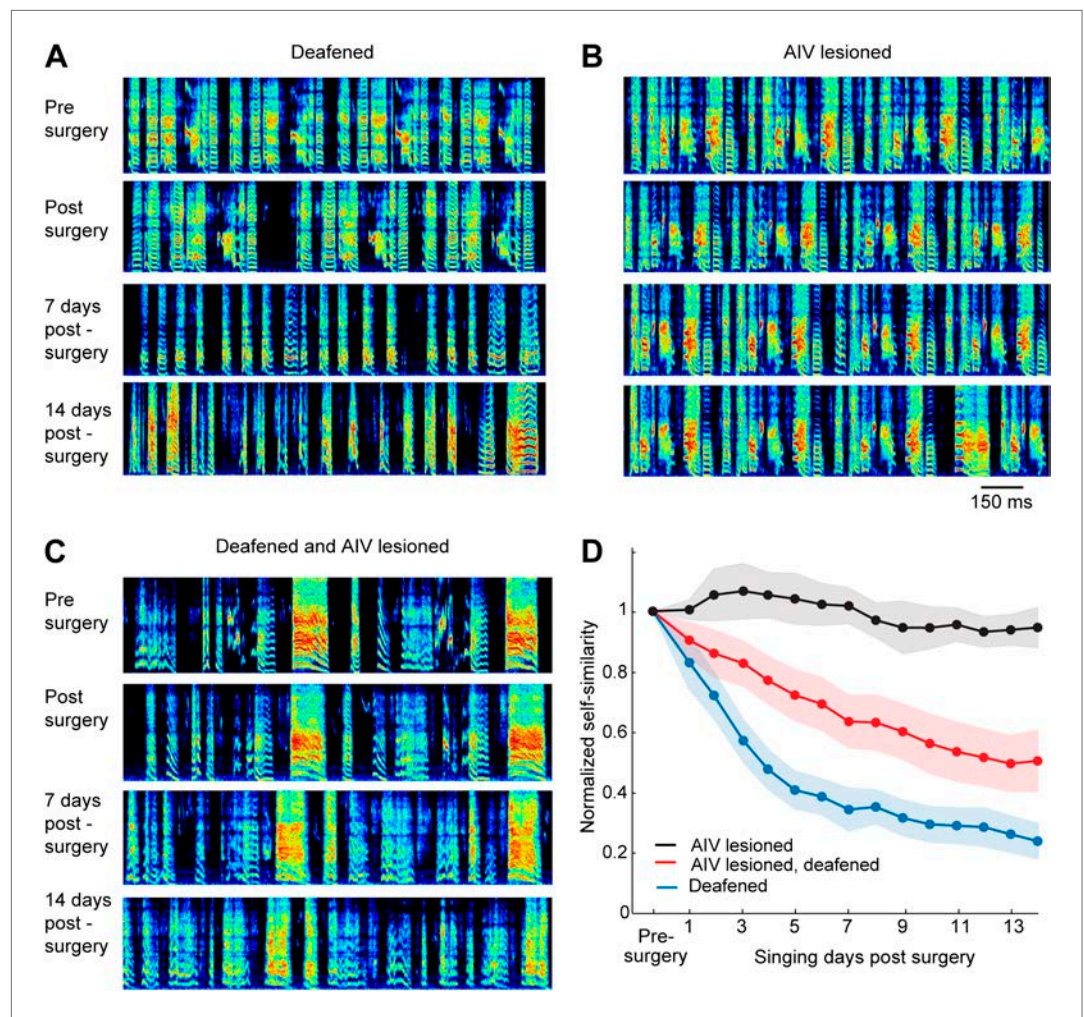


Figure 6. Effect of AIV lesion on adult song and on song degradation after deafening. **(A)** Examples of song spectrograms from a bird deafened at the age 80 dph. Shown from top to bottom; song before surgery (deafening), first song post-surgery, song 1 week post-surgery, and song 2 weeks post-surgery. Note rapid degradation of song structure within 1 week after deafening. **(B)** Examples of song spectrograms from a bird that underwent complete bilateral lesion of AIV at the age 80 dph. Note the lack of song degradation. **(C)** Song spectrograms from a bird that underwent both bilateral lesion of AIV and deafening at the age 80 dph. **(D)** Plot of song self-similarity, normalized to the average self-similarity of pre-surgery song. Note that lesioned birds exhibited a reduced rate of song degradation after deafening, compared to deafening alone, 1 week and 2 weeks post-surgery (t test, $p < 0.01$).

DOI: [10.7554/eLife.02152.012](https://doi.org/10.7554/eLife.02152.012)

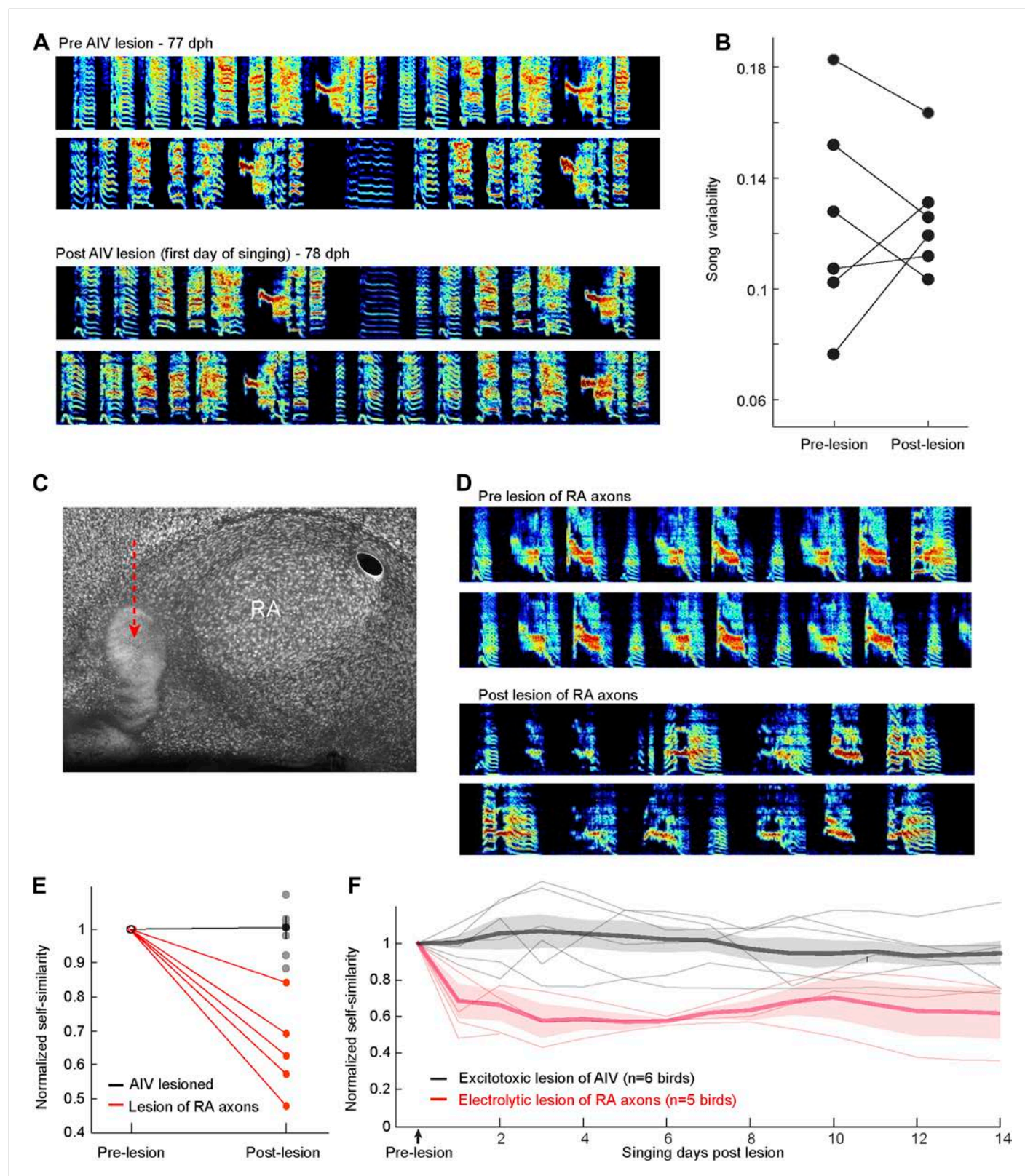


Figure 6—figure supplement 1. Immediate effects on song of excitotoxic and electrolytic lesions in AIV.

DOI: [10.7554/eLife.02152.013](https://doi.org/10.7554/eLife.02152.013)

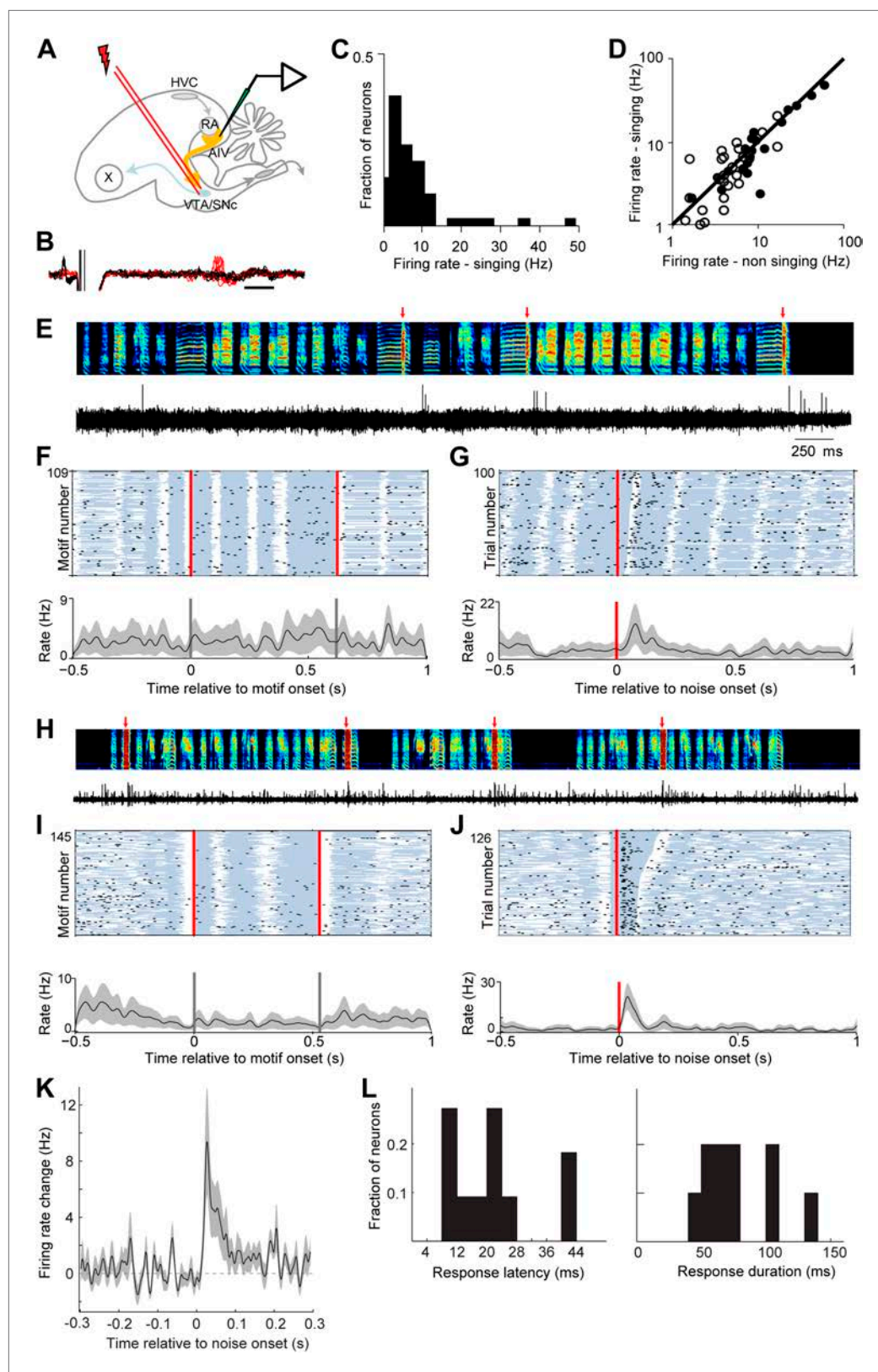


Figure 7. AIV neurons projecting to VTA/SNc exhibit error-related auditory responses during singing. (A) Schematic diagram of recording setup showing stimulating electrode placed in VTA/SNc for antidromic identification of AIV neurons. (B) Voltage traces showing an antidromically evoked spike of a VTA/SNc-projecting neuron. *Figure 7. Continued on next page*

Figure 7. Continued

AIV neuron (red spikes). Collision test shown in black traces. **(C)** Distribution of firing rates of AIV neurons during singing. **(D)** Firing rates of AIV neurons during singing vs non-singing (antidromically identified neurons, hollow circles; non-identified AIV neurons, filled circles). **(E)** Recording of an antidromically identified AIV neuron during singing (song spectrogram, top; extracellular voltage trace, bottom) with presentation of noise bursts (red arrows). **(F)** Motif-aligned spike raster plot of the AIV neuron from panel **E** during singing with no noise bursts presented. Each row in the raster plot corresponds to a rendition of the song motif. Each dot corresponds to a spike. Along each row, gray areas denote syllables and white areas denote silent gaps. Two vertical red lines denote motif onset and offset. Shaded area along the histogram denotes SEM. Note lack of singing-related firing rate modulations. **(G)** Spike raster plot and spike histogram aligned to noise bursts during singing. Red vertical line denotes noise onset. Other notations are as in **F**. Note the brief response to the noise burst during singing. **(H–J)** Another example of an antidromically identified AIV neuron (larger spike waveform) recorded during singing. **(I)** Motif-aligned raster plot of the AIV neuron from panel **H**. **(J)** Spike raster plot and histogram aligned to noise bursts during singing. Rasters are sorted by the duration of the syllable in which the noise burst occurred. Note that the response to noise burst occurs during different syllable types. **(K)** Average peri-stimulus histogram for all antidromically identified AIV neurons, aligned to noise burst onset during singing. **(L)** Distribution of response latency after noise burst (left) and response duration (right), for AIV neurons that showed a significant response to noise bursts.

DOI: [10.7554/eLife.02152.014](https://doi.org/10.7554/eLife.02152.014)

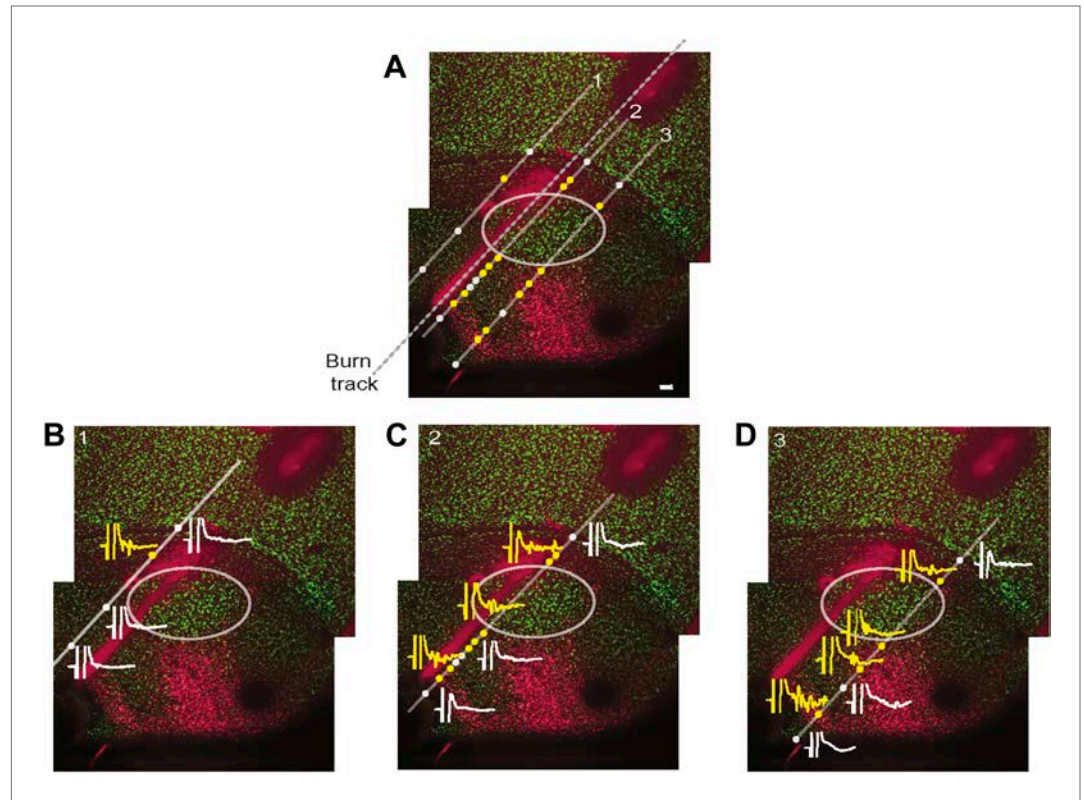


Figure 7—figure supplement 1. Simultaneous mapping of VTA/SNc-projecting neurons in AIV by antidromic activation and retrograde tracing.

DOI: [10.7554/eLife.02152.015](https://doi.org/10.7554/eLife.02152.015)

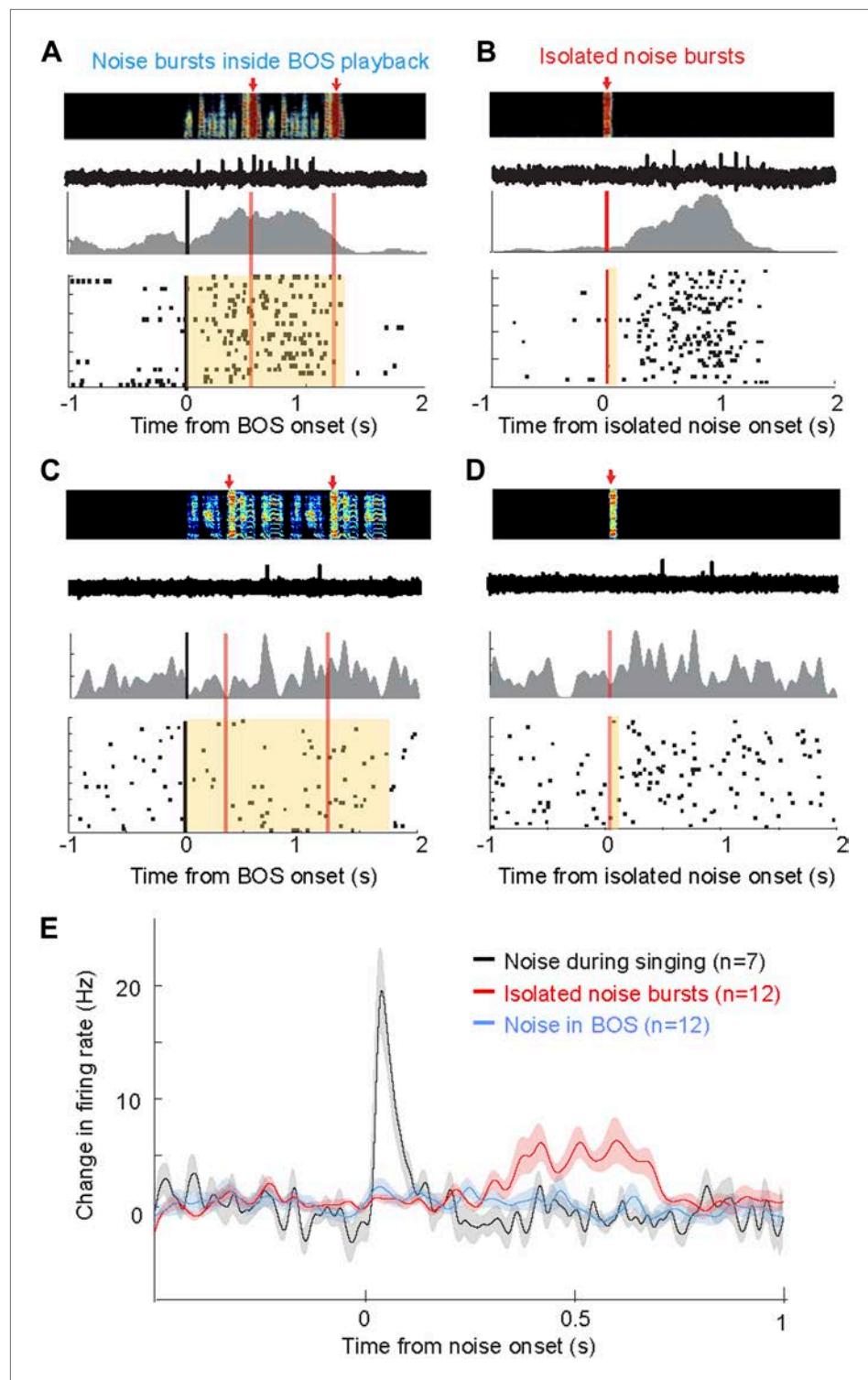


Figure 8. Response of AIV neurons to noise bursts during non-singing. **(A)** Activity of an antidromically identified AIV neuron recorded during presentation of noise bursts during playback of birds own song (BOS). Top to bottom panels: song spectrogram and simultaneous recording of neuronal activity; raster plot and spike histogram aligned to BOS onset (black line). Time of noise bursts indicated by vertical red lines. Yellow band denotes period of BOS playback. Note lack of response to noise bursts. **(B)** Response of the same neuron in panel **A** to presentation of isolated noise bursts (no BOS, no singing). Note slow timecourse of the response. **(C and D)** Recording of another antidromically identified AIV neuron (notation same as in panels **A** and **B**). **(E)** Averaged PSTH for all VTA/SNc-projecting AIV neurons. *Figure 8. Continued on next page*

Figure 8. Continued

that exhibited a significant response to isolated noise bursts within 1 s after noise onset. Average response of these same neurons to noise bursts presented during BOS playback (blue). In comparison, averaged response is shown for all VTA/SNc-projecting AIV neurons that responded significantly to noise burst during singing (black trace).

DOI: [10.7554/eLife.02152.016](https://doi.org/10.7554/eLife.02152.016)